Basic

Research Article

A pan-inflammatory microRNA-cluster is associated with orbital non-Hodgkin lymphoma and idiopathic orbital inflammation

Kamil G. Laban[1,2,3] 🆔 *, Rachel Kalmann*[1,2] *, Cornelis P. J. Bekker*[3,6] *, Sanne Hiddingh*[1,2,3] *,
Rob L. P. van der Veen*[2] *, Christine A. E. Eenhorst*[2] *, Stijn W. Genders*[4] *, Maarten P. Mourits*[5] *,
Fleurieke H. Verhagen*[1,2,3] 🆔 *, Emmerik F. A. Leijten*[3,6] *, Saskia Haitjema*[7] *, Mark C. H. de Groot*[7] *,
Timothy R. D. J. Radstake*[1,3,6] *, Joke H. de Boer*[1,2] *and Jonas J. W. Kuiper*[1,2,3]

[1] Ophthalmo-Immunology Unit, University Medical Center Utrecht, University Utrecht, Utrecht, The Netherlands
[2] Department of Ophthalmology, University Medical Center Utrecht, University Utrecht, Utrecht, The Netherlands
[3] Laboratory of Translational Immunology, University Medical Center Utrecht, University Utrecht, Utrecht, The Netherlands
[4] Department of Ophthalmology, Leiden University Medical Center, Leiden, The Netherlands
[5] Department of Ophthalmology, Academic Medical Center, Amsterdam, The Netherlands
[6] Department of Rheumatology & Clinical Immunology, University Medical Center Utrecht, University Utrecht, Utrecht, The Netherlands
[7] Laboratory of Clinical Chemistry and Haematology, University Medical Center Utrecht, Utrecht University, Utrecht, Netherlands

Non-Hodgkin orbital lymphoma (NHOL) and idiopathic orbital inflammation (IOI) are common orbital conditions with largely unknown pathophysiology that can be difficult to diagnose. In this study we aim to identify serum miRNAs associated with NHOL and IOI. We performed *OpenArray*® miRNA profiling in 33 patients and controls. Differentially expressed miRNAs were technically validated across technology platforms and replicated in an additional cohort of 32 patients and controls. We identified and independently validated a serum miRNA profile of NHOL that was remarkably similar to IOI and characterized by an increased expression of a cluster of eight miRNAs. Pathway enrichment analysis indicated that the miRNA-cluster is associated with immune-mediated pathways, which we supported by demonstrating the elevated expression of this cluster in serum of patients with other inflammatory conditions. The cluster contained *miR-148a*, a key driver of B-cell tolerance, and *miR-365* that correlated with serum IgG and IgM concentrations. In addition, *miR-29a* and *miR-223* were associated with blood lymphocyte and neutrophil populations, respectively. NHOL and IOI are characterized by an abnormal serum miRNA-cluster associated with immune pathway activation and linked to B cell and neutrophil dysfunction.

Keywords: B cell · idiopathic orbital inflammation · microRNA · neutrophil · non-hodgkin orbital lymphoma

🖥️ Additional supporting information may be found online in the Supporting Information section at the end of the article.

Correspondence: Kamil G. Laban
e-mail: K.G.laban@umcutrecht.nl

Introduction

Non-Hodgkin orbital lymphoma (NHOL) is the most common orbital malignancy in adults [1]. Early and accurate diagnosis is essential to reduce metastatic spread, and avoid disease-related morbidity and mortality. NHOL can be lethal without timely intervention, but prognosis varies across disease subtypes [2]. Generally, NHOL first presents as a non-specific mass within the orbit or ocular adnexa, which may be difficult to differentiate from *idiopathic orbital inflammation* (IOI), the most common non-thyroid associated orbital inflammatory condition [3–7]. Consequently, an incisional biopsy is required to accurately diagnose both diseases [1, 8]. However, a surgical biopsy can be technically challenging in case of deep orbital localization of the mass, which increases the risk for complications and nonrepresentative tissue biopsies. Therefore, less invasive tools to differentiate NHOL from inflammatory orbital disease are warranted. Although imaging-based disease differentiation is advancing [9], studies that explore blood-based differentiation of NHOL and IOI are scarce. Additionally, the pathophysiology of NHOL and IOI remain largely unknown.

MicroRNAs (miRNAs) are small non-coding regulatory RNAs that are present in almost all biological tissues and regulate gene expression by interfering with RNA translation [10]. Changes in the composition of miRNAs are associated with a plethora of human pathologies, including inflammation and cancer [11–13]. Consequently, miRNAs are candidate biomarkers that may aid in diagnosis and prognostic studies [14, 15]. Direct comparison of the serum miRNA profile of NHOL and IOI is currently lacking, but may provide a framework for understanding the miRNA composition of these orbital conditions for future differentiation and elucidation of the underlying mechanisms involved. In this exploratory study, we identify and validate NHOL- and IOI-related miRNA profiles in serum of two Dutch cohorts of patients and controls. In addition, we reference six non-orbital inflammatory conditions as disease controls to better understand miRNA expression changes.

Results

Patients

Demographics of the discovery and replication cohorts of are described in Table 1. Note, in both cohorts the mean age of the NHOL group was higher compared to the IOI and control groups, which is inherent to the representative age distribution for each of these conditions. In contrast, the mean age of the discovery and replication cohorts was similar for each orbital condition.

MiRNA analysis

To detect differences between NHOL, IOI, and healthy controls (HC), we performed a broad serum OpenArray® profiling of the discovery cohort (Fig. 1A). We detected 399 miRNAs of which 120 miRNAs remained after quality control (Supporting Information Table S1). Principle component analysis of the serum miRNA iden-

tified two samples that were considered technical outliers (Fig. 1B) that were excluded for further analysis because their expression levels strongly skewed group-level characteristics. In the remaining 31 samples, the overall miRNA expression was higher in the NHOL and IOI groups compared to the control group (Fig. 1C, Supporting Information Table S1). Head-to-head comparison of miRNA profiles between the investigated groups revealed several differentially expressed miRNAs (Fig. 2). The most differentially expressed miRNAs were found when comparing each of the orbital disease groups with controls. The mean levels of miRNAs were slightly higher in the IOI compared to NHOL group, but only U6 small nuclear RNA (*U6 snRNA*) exceeded the fold change (FC) >2.0 and $p < 0.05$ criterion (Fig. 2A). A total of 12 miRNAs were selected for technical validation (Supporting Information Table S2). This selected panel consisted of the most differentially expressed miRNAs (miR-29a-3p, miR-193a-5p, miR-223-3p, miR-223-5p, miR-148a-3p, miR-365a-3p, miR-143-3p, and U6 snRNA, see Fig. 2) and miR-140-5p, miR-215-5p, and miR-491-5p that are associated with inflammation and neoplasm [16–18], and highly correlated with the differentially expressed miRNAs (with a Spearman's $\rho > 0.75$). We also included miR-221-3p as a control in the validation phase, because this miRNA was not differentially expressed in the discovery cohort. The level of expression and variance of the selected miRNA panel considered for validation and replication was representative for the entire serum miRNA profile (i.e. not biased, Supporting Information Fig. S1). Analysis corrected for age and sex revealed no other miRNAs of interest for the comparison between NHOL and IOI.

A cluster of eight miRNAs is associated with NHOL and IOI

Having selected miRNAs of interest using the OpenArray® approach, we next aimed to validate the observations across technology platforms by measuring the levels of the twelve miRNAs using TaqMan single reverse transcription quantitative polymerase-chain reaction (RT-qPCR). We observed a strong correlation ($\rho > 0.75$; $p < 0.01$) between the expression levels obtained by OpenArray® and TaqMan RT-qPCR for 10/12 miRNAs, and considered these miRNAs technically validated (Fig. 3, Supporting Information Table S2). Next, we aimed to replicate our findings in a second cohort of 32 patients and controls (Table 1). We measured the levels of the technically validated miRNA in serum of the second (replication) cohort by RT-qPCR and observed that 8/10 miRNAs were differentially expressed between the groups with consistent direction of effect compared to HC. These eight miRNAs were considered biologically replicated. (Fig. 3, Supporting Information Table S2). Note that the expression levels of the biologically replicated miRNAs were significantly higher expressed in the disease groups compared to healthy controls (Fig. 3). Comparison of the data of the eight miRNAs revealed strong correlation of the expression levels, indicating co-expression, which we will further refer to as a 'cluster' of miRNAs in serum of patients (Fig. 4B).

Table 1. Cohort demographics

Discovery cohort	Discovery			Replication		
	IOI $n=14$	NHOL $n=10$	HC $n=9$	IOI $n=8$	NHOL $n=8$	HC $n=16$
Female (%)	2 (86%)	5 (50%)	6 (67%)	6 (75%)	5 (63%)	10 (63%)
Age (years); mean ± SD	48.7 ± 17.6	60.6 ± 9.7	47.1 ± 14.4	48.5 ± 17.2	64.9 ± 17.3	47.9 ± 10.7
NHOL subypte, n (%)						
EMZL	–	7 (70%)	–	–	4 (50%)	–
DLBCL	–	1 (10%)	–	–	1 (13%)	–
Follicular	–	1 (10%)	–	–	2 (25%)	–
Other	–	1 (10%)	–	–	1 (13%)	–

Abbreviations: IOI, idiopathic orbital inflammation; NHOL, non-Hodgkin orbital lymphoma; HC, healthy control; EMZL, extranodal marginal zone lymphoma; DLBCL, diffuse large B cell lymphoma.
Other NHOL types were a small lymphocytic lymphoma in the discovery cohort and a mantle-cell lymphoma in the replication cohort.

Next, we combined the RT-qPCR data from the discovery and replication cohorts to investigate the discriminative power of the miRNAs between the NHOL, IOI, and HC group. We observed a statistically significant discriminative power (area under the receiver operator curve range 0.72–0.92) with several cut-off values with FC < 2 for all miRNAs in the cluster for the diseased groups compared to the control group (Supporting Information Table S3). We observed a low discriminative power between NHOL and IOI, owing to the larger variation in expression in patients. However, the mean expression levels for miRNAs of the cluster were all slightly higher in IOI patients compared to NHOL (Fig. 4C). The expression levels of the eight miRNAs did not correlate with age and sex and consequently, correction for age and sex did not influence the outcome of the data.

The serum miRNA-cluster is typically increased in inflammatory disease

Since overall the miRNA-cluster showed the highest expression in IOI cases, we hypothesized that the cluster may regulate immune

pathways and would also be elevated in serum of cases with other chronic inflammatory conditions. To investigate this, we determined the expression of the cluster in serum of 57 patients with noninfectious uveitis [16], psoriasis, psoriatic arthritis, axial spondyloarthritis, and compared this to 26 unaffected controls. The serum miRNA profile for these conditions is outlined in Supporting Information Fig. S2. Interestingly, we observed that in general the miRNA-cluster was upregulated in these inflammatory conditions (Fig. 4A).

To explore the association of the miRNA-cluster with immune pathways in more detail, we used *miRTargetLink* [19] to extract putative gene targets of miRNA in the cluster. In total, 908 genes were reported to have evidence for interaction with any of the eight miRNAs. Pathway enrichment analysis was performed on the entire set of genes (*n = 908*) associated with this miRNA-cluster, and revealed enrichment for pathways related to cancer and inflammation, including mitogen-activated protein kinase signalling, p53 signalling, and interleukin signalling (Fig. 4D, and Supporting Information Fig. S3). A detailed pathway-enrichment analysis for each individual miRNA is outlined in Supporting Information Fig. S3.
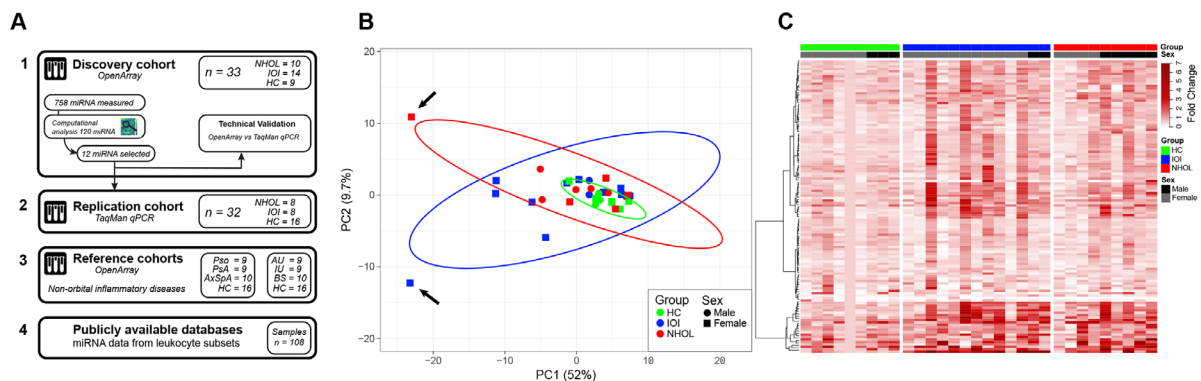

Figure 1. The serum miRNA profile of the discovery cohort. (A) Flowchart with the cohorts and technologies used in this study. (B) Principle component analysis with a projection of the first two components of all serum samples within the discovery cohort (*n = 33*). The ellipses represent the centre and the 95% confidence interval of the samples in each group. Two samples highlighted by black arrows were considered outliers and were excluded from further analysis. (C) Heatmap of the fold changes of spike-in normalized data compared to HC in expression of 120 serum miRNAs in the discovery cohort (*n = 31*). Relative miRNA expression is depicted in fold changes (FC, *or Singular Value Decomposition* imputed values, max 10%). Hierarchical clustering of the rows was performed using the Euclidian distance with Ward linkage method. Abbreviations: PC, principle component, IOI, idiopathic orbital inflammation; NHOL, non-Hodgkin orbital lymphoma; HC, healthy control.
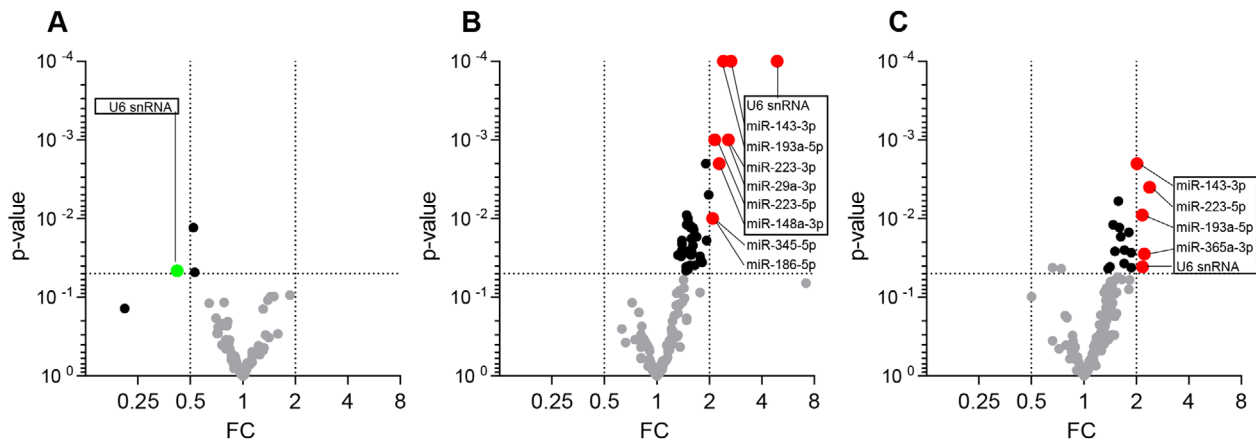
Figure 2. Volcano plot of head-to-head group comparisons for serum miRNAs in the discovery cohort. (A) The comparison between serum miRNA levels of the NHOL group ($n = 13$) and IOI group ($n = 9$). (B) The comparison between the IOI ($n = 13$) group with HC group ($n = 9$). (C) The comparison between the NHOL group ($n = 9$) and HC group ($n = 9$). Differentially expressed microRNAs are highlighted in green/red. The analysis was performed by independent samples t-test in the Thermo Fisher Cloud software. Differentially expressed miRNAs selected for replication are highlighted in boxes. Abbreviations: FC, fold change; IOI: idiopathic orbital inflammation; NHOL, non-Hodgkin orbital lymphoma; HC, healthy control.

The serum miRNA-cluster is associated with myeloid and lymphoid lineages

Having established the link between the miRNA-cluster and inflammation, we hypothesized that the expression levels of the miRNA-cluster in serum may inform on changes in the composition of blood leukocytes. To explore if the miRNA-cluster is associated with specific leukocyte populations in blood, we used miRNA profiling data of nine blood leukocyte populations ($n = 108$ samples). Considering the 12 selected miRNAs from the discovery cohort for principal component analysis, we observed that myeloid and lymphoid lineages could be distinguished primarily by the magnitude of difference of the levels of expression for *miR-223-3p* and *miR-29a-3p* (Fig. 4E). Indeed, *miR-223-3p* is predominantly expressed in monocyte, eosinophil, and neutrophil cells, while *miR-29a-3p* is more abundantly expressed in CD4$^+$ and CD8$^+$ T cells, B cells, and NK cells (Supporting Information Fig. S4). The increased expression of *miR-223-3p* and *miR-29a-3p* in certain leukocyte populations suggests that changes in leukocytes composition in blood may underlie the increase in the miRNA cluster in blood of patients with IOI and NHOL.

To test for associations between the blood leukocyte composition and serum miRNA levels, we evaluated the absolute frequency of several leukocyte populations in whole blood of both cohorts (Supporting Information Fig. S5A). Although the frequency of all leukocyte populations in available whole blood of patients was within normal range (Supporting Information Fig. S5A), NHOL patients showed a higher mean neutrophil cell size compared to IOI patients (Fig. 4F). In addition, the neutrophil cell size and serum *miR-223-3p* levels showed moderate positive correlation (Spearman's $\rho = 0.56$) in patients with IOI, but not in NHOL patients (Fig. 4G). These analyses suggest that the serum miRNA cluster is associated with neutrophil status in blood.

The levels of miR-365a-3p correlate with serum immunoglobulin

Inspired by the observations of miRNAs and the leukocyte composition, we compared the identified miRNA levels in serum with available clinical and demographic parameters relevant for orbital diseases. Correlation analysis revealed no association between the levels of each of the eight miRNAs and age or sex. We did observe a correlation between *miR-365a-3p* and serum Immunoglobulin-G and Immunoglobulin-M in NHOL and IOI patients at nominal significance (Supporting Information Table S4). No notable correlations were found between any of the eight miRNAs and C-reactive protein, erythrocyte sedimentation rate, rheumatoid factor, antinuclear antibodies, or soluble interleukin 2 levels.

Because B cells are implicated in both the aetiology of NHOL and orbital inflammation, we finally compared the expression of 19 miRNAs previously implicated in B cell autoimmunity and B cell lymphoma between IOI and NHOL [20]. This analysis revealed that the mean expression of B cell associated miRNAs in serum was similar between NHOL and IOI patients (Supporting Information Fig. S5B).

Discussion

In this study we discovered a remarkably similar miRNA profile for NHOL and IOI, and eight miRNAs were upregulated as part of a miRNA cluster in both NHOL and IOI compared to control. The eight miRNAs were found to be upregulated in several inflammatory diseases and related to inflammatory and oncological pathways.

With our results we show that local orbital disease leaves a molecular footprint in peripheral blood. This is consistent with other studies that reported changes in miRNA composition in tissues distinct from the primary location of clinical
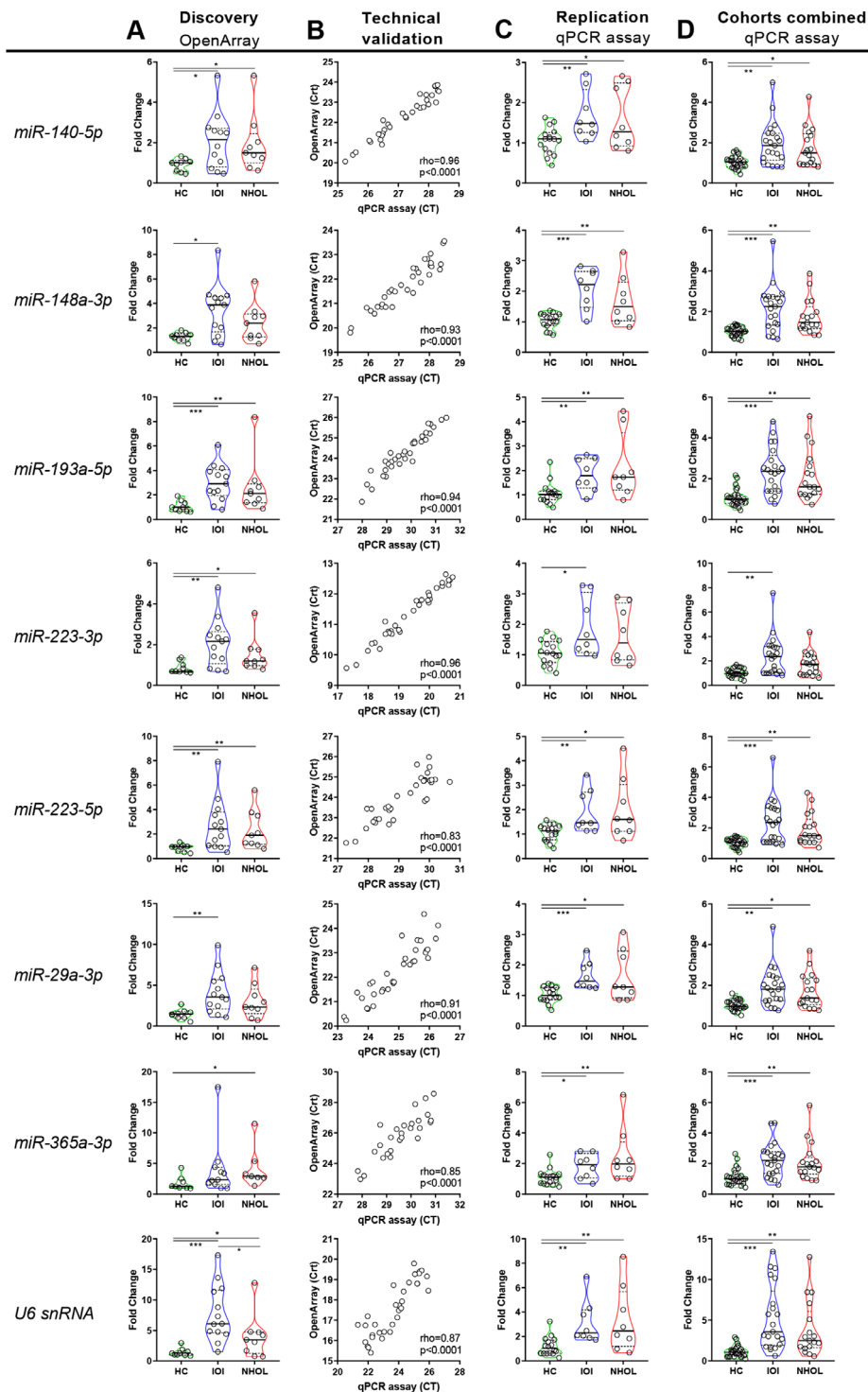
Figure 3. Eight serum microRNAs are increased in patients with NHOL and IOI. (A) miRNA expression of the Discovery cohort using OpenArray (*n* = 31). The relative expression of microRNAs is represented in fold changes (FC) of the diseased groups compared to healthy controls. *p*-values are calculated with an independent *t*-test on ΔΔCrt data. (B) Technical validation of the samples used for the OpenArray platform in a TaqMan single RT-qPCR assay. Technical validation was assessed using a Spearman's ρ correlation between Crt data (OpenArray) and Ct data (TaqMan RT-qPCR). (C) Results of the biological replication in an independent cohort using the TaqMan single RT-qPCR assay (*n* = 32). Relative expression is the fold change differences between the diseased groups and healthy control. Independent *t*-test is used on ΔΔCt data. (D) Results of the TaqMan single RT-qPCR of both cohorts (*n* = 63). Relative expression is the fold change differences between the diseased groups and the mean of the combined healthy control groups. Kruskal–Wallis statistics with post-hoc Dunn's test is used on ΔΔCt data. *p < 0.05, **p < 0.01, ***p < 0.001. Abbreviations: IOI, idiopathic orbital inflammation; NHOL, non-Hodgkin orbital lymphoma; HC, healthy control. The median expression is indicated for each group by a black line and quartiles with dotted lines.

disease [16, 21–23]. Previous studies have investigated miRNA profiles in non-Hodgkin lymphoma, most often the diffuse large B cell lymphoma subtype (DLBCL) [11, 14, 24]. DLBCL is a relative infrequent subtype of NHOL [2], reflected by only two cases in our study. In contrast, the most frequent NHOL subtype in our study was extranodal marginal zone lymohoma (EMZL), for which serum miRNAs studies are rare [11, 24]. Nonetheless, studies of lymphoma biopsies have shown an increased expression of *miR-223* and *miR-193* in EMZL [25], and a downregulation of *miR-29a*, *miR-223,* and *miR-140* in DLBCL [26]. This makes it tempting to speculate that the here-identified miRNA-cluster orchestrates pathological mechanisms associated with non-Hodgkin lymphoma, although the spatiotemporal miRNA expression may be dependent on the subtype of disease.

Additional analysis sheds light on the function of cluster of miRNAs: we demonstrate that the miRNAs associated with NHOL are
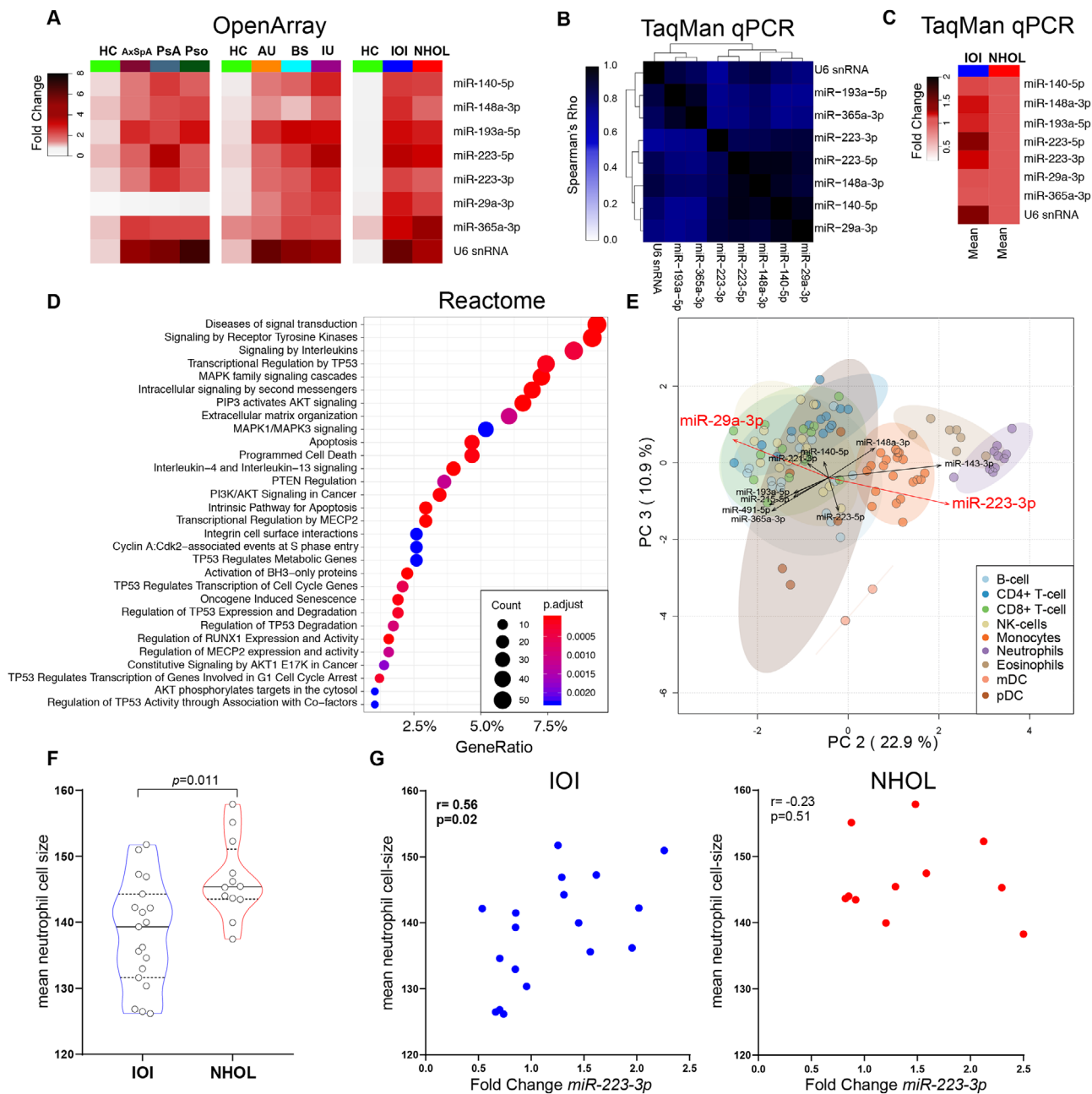
Figure 4. Investigation of the serum miRNA-cluster in inflammatory conditions and pathway enrichment analysis. (A) Heatmap of the validated miRNAs in independently analysed datasets of the investigated conditions and the referenced chronic inflammatory conditions (total samples $n = 113$). The relative miRNA expression per group is depicted as the mean fold changes compared to controls (HCs) and color-coded. (B) Correlation between the cluster of eight replicated miRNAs (all Spearman's ρ coefficients > 0.7, $p < 0.001$). Clustering of miRNA data was performed in *Metaboanalyst* of $\Delta\Delta$Ct data from TaqMan single RT-qPCR results of the discovery and replications cohorts of NHOL and IOI ($n = 63$). (C) Relative expression of the serum miRNA-cluster of TaqMan single RT-qPCR data from the discovery and replication cohorts ($n = 63$), depicted as mean fold change of IOI compared to NHOL. (D) Pathway enrichment analysis of 908 genes associated with the eight replicated miRNAs using the R package *clusterProfiler* with the *Reactome* database. The top 30 pathways are depicted (FDR adjusted *p*-value with a cut-off $p < 0.05$). (E) Principle component analysis (PCA) of miRNAs that were selected for replication in our study in 108 samples across nine blood leukocyte subsets. U6 snRNA was not available for this dataset. We excluded the first PCA dimension to reduce technical variation and batch effects. Individual loadings are projected over the individually plotted samples. Coloured ellipses represent the 95% confidence interval of the samples for each population. The *miR-223-3p* and *miR-29a-3p* showed the largest separation and are highlighted in red. (F) Violin plots of CELL-DYN Sapphire measured mean neutrophil size (0° Axial Light Loss) for the NHOL and IOI groups. The median bar (black line) and quartiles (dotted line) are shown within the violin plots. The Mann–Whitney *U* test was used for group comparison. (G) Pearson's correlation of relative expression of *miR-223-3p* and the mean neutrophil size within the NHOL and IOI groups are plotted separately. Abbreviations: IOI, idiopathic orbital inflammation; NHOL, non-Hodgkin orbital lymphoma; HC, healthy control; IU, idiopathic intermediate uveitis; AU, anterior uveitis; BS, Birdshot uveitis; AxSpA, axial spondyloarthritis; Pso, psoriasis; PsA, psoriatic arthritis; PC, principle component.

shared with a wide variety of chronic (orbital) inflammatory conditions, strongly suggesting that these miRNAs function in immune-mediated pathways and may be considered "pan-inflammatory". Indeed, pathway enrichment analysis for miRNA-target genes supports the hypothesis that these miRNAs regulate inflammatory and interleukin signalling. This is further supported by gene-expression studies of orbital biopsies that show interleukin, interferon, and TGF-signalling involvement [27, 28]. NHOL is driven by chromosomal translocations that drive B cell malignant growth [29] accompanied by chronic immune activation [30, 31]. The precise aetiology of IOI is unknown, yet B cell infiltration is also observed in IOI biopsies [27, 32]. Although the serum concentration of B cell associated miRNAs was similar between NHOL and IOI patients (Supporting Information Table S4), we observed that the mean levels of miRNAs in the identified cluster were slightly increased in IOI patients compared to NHOL. This increase is of interest because *miR-148a* and *miR-365* of the cluster are linked to specific B cell mechanisms. The microRNA *miR-148a* is a key regulator of B-cell tolerance and causes lethal autoimmune disease when increased in lupus-prone mice [33]. For *miR-365*, we observed that the expression correlated with serum IgG and IgM. *MiR-365* has been shown to regulate IL-6 signalling, which is important for B-cell differentiation [34]. Noteworthy, the levels of *miR-148a* and *miR-365* were not linked to the general B cell population (Supporting Information Fig. S4). Therefore, future studies on *miR-148a* and *miR-365* in specific B cell populations may aid in the differentiation of NHOL from IOI.

MiRNAs derived from leukocytes in blood are a major source of serum miRNAs and we observed that *miR-223-3p* and *miR-29a* were strongly associated with myeloid and lymphoid populations, respectively. A major source of *miR-223* in blood is neutrophils [35]. Although the neutrophil frequency in whole blood was not increased in patients with NHOL and IOI, we did observe that the neutrophil cell size in NHOL patients was higher compared to IOI. Note that the neutrophil cell size showed a wider ranger in IOI patients and exhibited a positive correlation with the serum levels of *miR-223-3p* in serum of IOI patients. As we observe a 'pathological' increase of *miR-223-3p* in orbital disease, the increased neutrophil cell size could therefore be related to disease mechanisms. For example, blood neutrophil size increases after stimulation with various agonists [36]. Neutrophils are known to infiltrate lymphoma tissues where they can produce APRIL, a potent factor that can induce B cell neoplasia and is linked to tumor aggressiveness and disease outcome [37]. Alternatively, neutrophils have been shown to protect lymphoma B cells against chemotherapeutic agents by direct cell interaction [38]. These neutrophil functions support a role for neutrophils in NHOL, but follow-up studies on the relation between *miR-223* and neutrophils in NHOL are warranted. This relation may be of interest since the serum levels of *miR-223* have been linked with poor cancer prognosis [39]. Considering these associations, more detailed investigation of circulatory cellular compartments and neutrophil populations could reveal changes in other leukocyte populations that may differentiate NHOL from IOI. The lack of association between miRNA levels and other clinical parameters

may in part be caused by heterogeneity among patients. We noted that the expression of cluster miRNAs was highly variable amongst patients. Better understanding of this heterogeneity and the link to disease outcomes may provide opportunities to conduct personalized therapy adjustments or prognosis predictions.

Using discovery, technical validation and independent replication of serum miRNAs we showed high concordance of the OpenArray® with targeted RT-qPCR. Although the *Area Under the Receiver Operating Characteristics* suggest that subtle changes in miRNA levels in serum (FC<2) may be relevant to distinguish patients from controls (Supporting Information Table S3), we show that reproducible changes in miRNAs are the best in those with FC > 2. This suggests a limitation of the OpenArray® platform, as it may be less sensitive to accurately detect subtle differences in miRNA expression, and small RNA sequencing would be more appropriate to further investigate other candidates. We aimed to identify miRNAs that were distinct between NHOL and IOI, but identified strong disease signatures that were shared by these conditions.

NHOL covers several disease subtypes with varying disease course and underlying molecular circuitry [1]. Most NHOL were of the EMZL subtype in this study (Table 1) and we were therefore unable to compare NHOL subtypes. Previously, a comparison of miRNA profiles in NHOL tissue of EMZL and DLBCL have been found to differ [40], although this was not compared in peripheral blood and did not include a control group. Three NHOL patients included in this study had a history of lymphoma in remission. Although they could be considered secondary NHOL, their results were comparable to the NHOL group as a whole and were not considered outliers within the data. Idiopathic conditions such as IOI that are diagnosed based on exclusion may show relatively high variability of disease characteristics, which would require large sample size to dissect disease endotypes to better differentiate these from NHOL. The variability within the IOI population is supported by previous gene expression studies that suggest overlap between an IOI subgroup and disease such as GPA [28]. However, IOI remains a clinical entity [7], classically treated with oral immunosuppressant therapy [4, 6].

Our study suggests that serum miRNAs analysed by the OpenArray® platform provide no feasible clinical biomarkers to differentiate NHOL from IOI. However, the results of the current study should be considered a stepping-stone into deeper understanding the close relation between these orbital pathologies and guide future studies that use molecular phenotyping for differentiation. For future studies we would recommend the use of functional experiments for the miRNA cluster found in this study. Additionally, peripheral blood immune-phenotyping could reveal cell-types of interest for differentiation of NHOL and IOI.

In conclusion, we observed overlapping serum miRNA profiles between NHOL and IOI, and identified a pan-inflammatory miRNA-cluster upregulated in patients of both diseases compared to controls. The findings of this study bring new insights in the complex and possibly overlapping pathophysiology of NHOL and IOI.

Materials and methods

Ethical considerations

This cross-sectional case-control study was conducted in compliance with the Helsinki principles. Ethical approval was requested and obtained from the local Medical Ethical Research Committee in Utrecht and all patients signed written informed consent before participation.

Discovery and replication cohorts

In total, 40 NHOL ($n = 18$) and IOI ($n = 22$) patients and 25 unaffected controls (HC) were included in this study (Fig. 1A). All patients were recruited at the department of Ophthalmology at the University Medical Center Utrecht, Utrecht, The Netherlands between February 2015 and May 2018. We performed serum miRNA experiments in a discovery cohort (NHOL: $n = 10$, IOI: $n = 14$, HC: $n = 9$) and one year later a replication cohort (NHOL: $n = 8$, IOI: $n = 8$; HC: $n = 16$).

All patients were diagnosed by an ophthalmologist specialized in orbital diseases. NHOL patients were diagnosed following WHO criteria with histopathological assessment of incisional biopsies [41]. Within the histopathologic examination, the pathologist assessed B and T cell specific markers (CD3, CD5, CD20, CD79α) and specific B cell subset markers (BCL2, BCL6, CD10, CD23, CD30, Cyclin D-1, MUM-1, and κ and λ light chains) for NHOL subtyping. Additional molecular analysis included PCR to assess monoclonality in all but two biopsies and translocations were assessed by fluorescence in situ hybridization in patients with DLBCL.

IOI were diagnosed based on exclusion of infection, specific orbital inflammatory disorder (e.g. thyroid eye disease, granulomatosis with polyangiitis (former Wegener's disease), sarcoidosis, primary Sjögren's syndrome, benign lymphoid hyperplasia, histiocytic disease or IgG4-related pathology), or malignant neoplasia based on consensus criteria [7, 8]. Histopathological confirmation of incisional biopsies was obtained in all patients, except in patients with idiopathic myositis ($n = 6$). All IOI biopsies revealed a non-specific polymorphous plasmalymphocytic infiltrate, negative for IgG4, with or without the presence of neutrophils, eosinophils, histiocytes, and macrophages, and varying amounts of fibrosis in the connective tissue. Idiopathic myositis was diagnosed based on the presence of pain, diplopia, (paretic) motility reduction, and pain with eye-movement, negative laboratory findings (e.g. negative antibodies and normal serum IgG4 levels) and extra-ocular muscle swelling with contrast-enhancement on *magnetic resonance imaging* [7].

All patients had blood withdrawal at the time of diagnosis in active disease and before treatment initiation. Additionally, none of the patients received systemic corticosteroids three months — or immunomodulatory treatment in the last six months — prior to blood withdrawal, except for one patient of the validation cohort (low dose of 2.5 mg oral prednisolone daily). Also, patients had not received radiation treatment or chemotherapy in the last year before sampling. A total of 25 anonymous blood-donors with no history of inflammatory disease or malignancies were included as an unaffected control group.

Reference cohorts

To assess specificity for orbital disease associated miRNAs, we included local and systemic inflammatory reference groups of which OpenArray® miRNA data was available in our center. OpenArray® data were obtained for 28 patients with anterior uveitis, idiopathic intermediate uveitis, and Birdshot uveitis, and 16 controls from a recent serum miRNA profiling study [16]. In addition, we collected serum from 29 patients with psoriasis, psoriatic arthritis, axial spondyloarthritis, and 10 controls, of which data has not been published previously and therefore described in more detail. Briefly, patients were recruited from the Department of Rheumatology & Clinical Immunology of the University Medical Center Utrecht, Utrecht, The Netherlands with active disease and were free from systemic immunomodulatory treatment at the time of blood withdrawal. Psoriasis patients were diagnosed by dermatologists with a consultation by a rheumatologist. Psoriatic arthritis was classified by a rheumatologist following the CASPAR criteria [42], and axial spondyloarthritis was classified by a rheumatologist in accordance with Assessment of SpondyloArthritis International Society classification criteria [43].

OpenArray® profiling

Blood was drawn in serum tubes containing separating gel and clot activator (BD Vacutainer), rested for 30 min at room temperature and centrifuged for 10 min at $2000 \times g$. Serum was isolated and stored at $-80°C$ until measurements were performed as previously described by *Verhagen et al. 2018* [16]. In brief, RNA was extracted from 200 μL serum using Exiqon's MiRCURY™ RNA Isolation Kit for biofluids (Exiqon, Denmark), according to manufacturer's instructions. We used non-human miRNA (*ath-miR-159a*) as spike-in control for normalization in data-analysis. Screening for miRNAs was performed using Taqman real-time PCR on the OpenArray® platform (Thermo Fisher Scientific, USA) according to manufacturer's instruction. With this technique, a total of 758 miRNAs could be screened in two primer pools, pool A and pool B (Life Technologies). Reverse transcription (RT) was performed on 2.5 μL isolated RNA using multiplex RT primers (v2.1 for pool A and v3.0 for pool B) and the TaqMan miRNA RT kit (Thermo Fisher Scientific, USA). Megaplex™ PreAmp Primers and TaqMan PreAmp Master Mix (Themo Fisher Scientific, USA) were used for preamplification of RT products with the following thermal cycler conditions: 10 min at 95°C, 2 min at 55°C, 2 min at 72°C, 16 cycles of 15 sec at 95°C, and 4 min at 60°C, followed by a single cycle of 10 min at 96°C (Biometra® Thermocycler). The pre-amplified products were diluted (1:40) in 0.1xTE buffer (pH 8) and (1:2) with the TaqMan OpenArray® Real-Time PCR Master Mix. MiRNA profiling was performed on the QuantStudio 12 K

Flex Real-Time PCR system (Thermo Fisher Scientific, USA). The miRNA expression levels were analysed using the ThermoFisher Cloud software v1.0 (www.thermofisher.com). Samples with an amplification score <1.25 were excluded and the expression levels converted to the platforms relative cycle threshold (Crt) values. MiRNAs with a mean Crt > 27 were considered to be below the detection level and excluded from further analysis. For the included miRNAs (mean Crt < 27 in all samples), individual samples with Crt > 27 were set to Crt = 27. We excluded miRNAs for further analysis if these were detected in <80% of all samples. The relative expression was defined as the ΔCrt value, which is calculated to normalize the data by subtraction the mean Crt-value of the spike-in control from the mean Crt for each miRNA (ΔCrt = $Crt_{mean\ target}$ – $Crt_{mean\ spike-in}$). Differences in miRNA expression levels were assessed comparing the comparative threshold cycle method [44]. Relative miRNA expression levels are presented as Fold Change (FC = $2^{-\Delta\Delta Crt}$, where $\Delta\Delta Crt = \Delta Crt_{sample}$ - $\Delta Crt_{reference}$) with a mean ΔCrt of the control group as reference (set at mean FC = 1). We considered differentially expressed miRNAs with a threshold values of FC > 2.0 and $p < 0.05$. We selected miRNAs for validation based on a combination of the highest FC difference and lowest p-values between the study groups, and strong correlations. A non-differentially expressed miRNA was taken along as control.

Single RT-qPCR assay for validation

Single TaqMan RT-qPCR was performed for 12 miRNAs selected for validation (Supporting Information Table S2). The cDNA was synthesized from 2.5μL RNA using individual miRNA-specific stem-loop primers according to manufacturer's instructions in the presence of 3.3 U/μL MultiScribe RT enzyme (Thermo Fisher). After addition of the TaqMan Fast Advance Master Mix and specific primers, miRNA expression was quantified in duplicate using the QuantStudio 12 K Flex Real-Time PCR system. *Anth-miR-159a* was used as the spike-in control. Technical validation was defined as strong correlation (Spearman's ρ correlation > 0.75 and $p < 0.05$) between Ctr values from the OpenArray and cycle threshold (Ct) values from the RT-qPCR assay for each individual miRNA target. Next, technically validated miRNAs were independently assessed using a second cohort ($n = 32$) for biological replication. Analysis of relative miRNA expression for the RT-qPCR assay was similar to the analysis of the OpenArray® profiling, using the median ΔCt value for the control group as a reference (set at 1).

Statistical analysis

The discovery cohort analysis of the OpenArray® profiling was performed within the Thermo Fisher Cloud software and the replication cohort using IBM SPSS Statistics for Windows, Version 25.0, released in 2017 (Armonk, NY: IBM Corp). The Thermo Fisher Cloud software exploits an independent samples t-test to compare $\Delta\Delta$Crt data to one randomly selected representative reference control sample using a two-tailed p-value threshold of 0.05. For technical validation of the discovery cohort for OpenArray® and RT-qPCR array data we used the Spearman rank correlation test. For comparison with the discovery cohort we used an independent samples t-test for the replication cohort. For the analysis of the combined discovery and replication cohorts we used the Kruskal–Wallis test with post-hoc Dunn's correction to adjust p-values. Additionally, a Benjamini–Hochberg correction was deployed on the combined cohort results to correct for multiple testing [45]. We associated miRNA expression with clinical characteristics (Supporting Information Table S4) using the $\Delta\Delta$Ct of the combined analysis (both cohorts). Principal component analysis and hierarchical cluster analysis of the OpenArray® data were conducted using the MetaboAnalyst servers v4.0 or the heatmap.2 function in the R *gplot* package [46]. GraphPad Prism (GraphPad, La Jolla, CA, USA) was used for violin- and volcanoplots.

MiRNA gene target analysis

Target genes of the validated miRNAs were mapped using *miRTargetLink* [19]. The R package *clusterProfiler* was used for pathway enrichment analyses [47], exploiting the *Kyoto Encyclopaedia of Genes and Genomes* (KEGG) pathways [48] and *Reactome Pathway Knowledgebase* [49] databases.

MiRNA profiling in circulatory leukocyte cell subsets

Global MicroRNA expression data of nine primary purified leukocyte populations were derived from four non-coding RNA microarray data sets available via the Gene Expression Omnibus public repository of the NCBI (accession no. GSE19183, GSE28487, GSE28489, GSE98830). The FACS-sorted populations were obtained from 12 unaffected controls and include multiple populations from the same individuals. Raw data scans (.CEL files) were read into R (R version 3.3.2). Samples were preprocessed with Affy package version 3.3.1 for Affymetrix Multispecies miRNA-1 Array and Limma package version 3.3.3 for Agilent-021827 Human miRNA Microarray. A total of 825 overlapping human micro-RNAs for 108 samples were pooled and quantile-normalized. A principle component analysis was performed to interrogate miRNA expression profiles for the selected miRNAs of the validation phase (except for U6 snRNA that was not available within the dataset) using MetaboAnalyst 3.05 with the exception of the first component to reduce technical variation and batch effect [50].

Whole blood leukocyte counts

Leukocyte counts, leukocyte subset counts, as well as leukocyte cell size and leukocyte complexity in blood were obtained for most patients from routine analysis of whole blood samples by the CELL-DYN Sapphire (Abbott Diagnostics, Santa Clara, CA, USA), an automated routine haematology analyser that uses spectrophotometry, electrical impedance, and laser light scattering [51]. The

neutrophil cell size and complexity were determined by optical scatter using 0° Axial Light Loss for cell size and 7° Intermediate Angle Scatter for complexity. CELL-DYN data from the Utrecht Patient Oriented Database (UPOD) were used. UPOD is an infrastructure of relational databases comprising data on patient characteristics, hospital discharge diagnoses, medical procedures, medication orders, and laboratory tests for all patients treated at the University Medical Center Utrecht, Utrecht, The Netherlands since 2004. UPOD data acquisition and management is in accordance with current regulations concerning privacy and ethics. The structure and content of UPOD have been described in more detail elsewhere [52].

Conflict of interest: The authors declare no financial or commercial conflict of interest.

References

1 **Olsen, T. G. and Heegaard, S.,** Orbital lymphoma. *Surv. Ophthalmol.* 2019. **64**: 45–66.

2 **Olsen, T. G., Holm, F., Mikkelsen, L. H., Rasmussen, P. K., Coupland, S. E., Esmaeli, B., Finger, P. T. et al.,** Orbital lymphoma—an international multicenter retrospective study. *Am. J. Ophthalmol.* 2019. **199**: 44–57.

3 **Ben Simon, G. J., Cheung, N., McKelvie, P., Fox, R. and McNab, A. A.,** Oral chlorambucil for extranodal, marginal zone, B-cell lymphoma of mucosa-associated lymphoid tissue of the orbit. *Ophthalmology* 2006. **113**: 1209–13.

4 **Yuen, S. J. A. and Rubin, P. A. D.,** Idiopathic orbital inflammation: distribution, clinical features, and treatment outcome. *Arch. Ophthalmol. (Chicago, Ill. 1960).* 2003. **121**: 491–9.

5 **Yan, J., Wu, Z. and Li, Y.,** The differentiation of idiopathic inflammatory pseudotumor from lymphoid tumors of orbit: analysis of 319 cases. *Orbit* 2004. **23**: 245–54.

6 **Gordon, L. K.,** Orbital inflammatory disease: a diagnostic and therapeutic challenge. *Eye* 2006. **20**: 1196–1206.

7 **Mombaerts, I., Bilyk, J. R., Rose, G. E., McNab, A. A., Fay, A., Dolman, P. J., Allen, R. C. et al.,** Consensus on diagnostic criteria of idiopathic orbital inflammation using a modified delphi approach. *JAMA Ophthalmol.* 2017. **135**: 769–776.

8 **Mombaerts, I., Rose, G. E. and Garrity, J. A.** Orbital inflammation: biopsy first. *Surv. Ophthalmol.* 2016. **61**: 664–669.

9 **Hiwatashi, A., Togao, O., Yamashita, K., Kikuchi, K., Kamei, R., Yoshikawa, H., Takemura, A. et al.,** Diffusivity of intraorbital lymphoma vs. inflammation: comparison of single shot turbo spin echo and multishot echo planar imaging techniques. *Eur. Radiol.* 2018. **28**: 325–330.

10 **Baek, D., Villén, J., Shin, C., Camargo, F. D., Gygi, S. P. and Bartel, D. P.,** The impact of microRNAs on protein output. *Nature* 2008. **455**: 64–71.

11 **Solé, C., Arnaiz, E. and Lawrie, C. H.,** MicroRNAs as biomarkers of B-cell lymphoma. *Biomark. Insights.* 2018. **13**: 117727191880684. https://doi.org/10.1177/1177271918806840.

12 **Marques-Rocha, J. L., Samblas, M., Milagro, F. I., Bressan, J., Martínez, J. A. and Marti, A.,** Noncoding RNAs, cytokines, and inflammation-related diseases. *FASEB J.* 2015. **29**: 3595–611.

13 **Mi, S., Zhang, J., Zhang, W. and Huang, R. S.,** Circulating microRNAs as biomarkers for inflammatory diseases. *MicroRNA (Shariqah, United Arab Emirates).* 2013. **2**: 63–71.

14 **Larrabeiti-Etxebarria, A., Lopez-Santillan, M., Santos-Zorrozua, B., Lopez-Lopez, E. and Garcia-Orad, A.,** Systematic review of the potential of microRNAs in diffuse large B cell lymphoma. *Cancers (Basel).* 2019. **11**: 144.

15 **Tuo, J., Shen, D., Yang, H. H. and Chan, C.-C.,** Distinct microRNA-155 expression in the vitreous of patients with primary vitreoretinal lymphoma and uveitis. *Am. J. Ophthalmol.* 2014. **157**: 728–34.

16 **Verhagen, F. H., Bekker, C. P. J., Rossato, M., Hiddingh, S., de Vries, L., Devaprasad, A., Pandit, A. et al.,** A disease-associated microRNA cluster links inflammatory pathways and an altered composition of leukocyte subsets to noninfectious uveitis. *Invest. Ophthalmol. Vis. Sci.* 2018. **59**: 878–888..

17 **Singh, A., Bhattacharyya, N., Srivastava, A., Pruett, N., Ripley, R. T., Schrump, D. S. and Hoang, C. D.,** MicroRNA-215-5p treatment suppresses mesothelioma progression via the MDM2-p53-signaling axis. *Mol. Ther.* 2019. **27**: 1665–1680.

18 **Zhang, Q., Weng, Y., Jiang, Y., Zhao, S., Zhou, D. and Xu, N.,** Overexpression of miR-140-5p inhibits lipopolysaccharide-induced human intervertebral disc inflammation and degeneration by downregulating toll-like receptor 4. *Oncol. Rep.* 2018. **40**: 793–802.

19 **Hamberg, M., Backes, C., Fehlmann, T., Hart, M., Meder, B., Meese, E. and Keller, A.,** miRTargetLink—miRNAs, genes and interaction networks. *Int. J. Mol. Sci.* 2016. **17**: 564.

20 **Zheng, B., Xi, Z., Liu, R., Yin, W., Sui, Z., Ren, B., Miller, H. et al.,** The function of microRNAs in B-cell development, lymphoma, and their potential in clinical practice. *Front. Immunol.* 2018. **9**: 936.

21 **Khoury, S. and Tran, N.,** Circulating microRNAs: potential biomarkers for common malignancies. *Biomark. Med.* 2015. **9**: 131–151.

22 **Correia, C. N., Nalpas, N. C., McLoughlin, K. E., Browne, J. A., Gordon, S. V., MacHugh, D. E. and Shaughnessy, R. G.,** Circulating microRNAs as potential biomarkers of infectious disease. *Front. Immunol.* 2017. **8**: 118.

23 **Backes, C., Meese, E. and Keller, A.,** Specific miRNA disease biomarkers in blood, serum and plasma: challenges and prospects. *Mol. Diagn. Ther.* 2016. **20**: 509–518.

24 **Fernandez-Mercado, M., Manterola, L. and Lawrie, C.,** MicroRNAs in lymphoma: regulatory role and biomarker potential. *Curr. Genomics* 2015. **16**: 349–358.

25 **Arribas, A. J.**, **Campos-Martín, Y.**, **Gómez-Abad, C.**, **Algara, P.**, **Sánchez-Beato, M.**, **Rodriguez-Pinilla, M. S.**, **Montes-Moreno, S. et al.**, Nodal marginal zone lymphoma: gene expression and miRNA profiling identify diagnostic markers and potential therapeutic targets. *Blood* 2012. **119**: e9–e21.

26 **Caramuta, S.**, **Lee, L.**, **Ozata, D. M.**, **Akçakaya, P.**, **Georgii-Hemming, P.**, **Xie, H.**, **Amini, R.-M. et al.**, Role of microRNAs and microRNA machinery in the pathogenesis of diffuse large B-cell lymphoma. *Blood Cancer J.* 2013. **3**: e152.

27 **Wladis, E. J.**, **Iglesias, B. V. and Gosselin, E. J.**, Characterization of the molecular biologic milieu of idiopathic orbital inflammation. *Ophthalmic Plast. Reconstr. Surg.* 2011. **27**: 251–254.

28 **Rosenbaum, J. T.**, **Choi, D.**, **Wilson, D. J.**, **Grossniklaus, H. E.**, **Harrington, C. A.**, **Sibley, C. H.**, **Dailey, R. A. et al.**, Orbital pseudotumor can be a localized form of granulomatosis with polyangiitis as revealed by gene expression profiling. *Exp. Mol. Pathol.* 2015. **99**: 271–278.

29 **Takahashi, H.**, **Usui, Y.**, **Ueda, S.**, **Yamakawa, N.**, **Sato-Otsubo, A.**, **Sato, Y.**, **Ogawa, S. et al.**, Genome-wide analysis of ocular adnexal lymphoproliferative disorders using high-resolution single nucleotide polymorphism array. *Invest. Ophthalmol. Vis. Sci.* 2015. **56**: 4156–65.

30 **Makgoeng, S. B.**, **Bolanos, R. S.**, **Jeon, C. Y.**, **Weiss, R. E.**, **Arah, O. A.**, **Breen, E. C.**, **Martínez-Maza, O. et al.**, Markers of immune activation and inflammation, and non-hodgkin lymphoma: a meta-analysis of prospective studies. *JNCI cancer Spectr.* 2018. **2**: pky082.

31 **Smedby, K. E. and Ponzoni, M.**, The aetiology of B-cell lymphoid malignancies with a focus on chronic inflammation and infections. *J. Intern. Med.* 2017. **282**: 360–370.

32 **Ho, V. H.**, **Chevez-Barrios, P.**, **Jorgensen, J. L.**, **Silkiss, R. Z.**, **Silkis, R. Z. and Esmaeli, B.**, Receptor expression in orbital inflammatory syndromes and implications for targeted therapy. *Tissue Antigens* 2007. **70**: 105–9.

33 **Gonzalez-Martin, A.**, **Adams, B. D.**, **Lai, M.**, **Shepherd, J.**, **Salvador-Bernaldez, M.**, **Salvador, J. M.**, **Lu, J. et al.**, The microRNA miR-148a functions as a critical regulator of B cell tolerance and autoimmunity. *Nat. Immunol.* 2016. **17**: 433–40.

34 **Xu, Z.**, **Xiao, S.-B.**, **Xu, P.**, **Xie, Q.**, **Cao, L.**, **Wang, D.**, **Luo, R. et al.**, miR-365, a novel negative regulator of interleukin-6 gene expression, is cooperatively regulated by Sp1 and NF-κB. *J. Biol. Chem.* 2011. **286**: 21401–21412.

35 **Tsitsiou, E. and Lindsay, M. A.**, microRNAs and the immune response. *Curr. Opin. Pharmacol.* 2009. **9**: 514–20.

36 **Bashant, K. R.**, **Vassallo, A.**, **Herold, C.**, **Berner, R.**, **Menschner, L.**, **Subburayalu, J.**, **Kaplan, M. J. et al.**, Real-time deformability cytometry reveals sequential contraction and expansion during neutrophil priming. *J. Leukoc. Biol.* 2019. https://doi.org/10.1002/JLB.MA0718-295RR.

37 **Schwaller, J.**, **Schneider, P.**, **Mhawech-Fauceglia, P.**, **McKee, T.**, **Myit, S.**, **Matthes, T.**, **Tschopp, J. et al.**, Neutrophil-derived APRIL concentrated in tumor lesions by proteoglycans correlates with human B-cell lymphoma aggressiveness. *Blood* 2007. **109**: 331–8.

38 **Hirz, T.**, **Matera, E.-L.**, **Chettab, K.**, **Jordheim, L. P.**, **Mathé, D.**, **Evesque, A.**, **Esmenjaud, J. et al.**, Neutrophils protect lymphoma cells against cytotoxic and targeted therapies through CD11b/ICAM-1 binding. *Oncotarget* 2017. **8**: 72818–72834.

39 **Li, Z.**, **Yang, Y.**, **Du, L.**, **Dong, Z.**, **Wang, L.**, **Zhang, X.**, **Zhou, X. et al.**, Overexpression of miR-223 correlates with tumor metastasis and poor prognosis in patients with colorectal cancer. *Med. Oncol.* 2014. **31**: 256.

40 **Hother, C.**, **Rasmussen, P. K.**, **Joshi, T.**, **Reker, D.**, **Ralfkiær, U.**, **Workman, C. T.**, **Heegaard, S. et al.**, MicroRNA profiling in ocular adnexal lymphoma: a role for MYC and NFKB1 mediated dysregulation of microRNA expression in aggressive disease. *Invest. Ophthalmol. Vis. Sci.* 2013. **54**: 5169–75.

41 **Swerdlow, S. H.**, **Campo, E.**, **Pileri, S. A.**, **Harris, N. L.**, **Stein, H.**, **Siebert, R.**, **Advani, R. et al.**, The 2016 revision of the World Health Organization classification of lymphoid neoplasms. *Blood* 2016. **127**: 2375–2390.

42 **Taylor, W.**, **Gladman, D.**, **Helliwell, P.**, **Marchesoni, A.**, **Mease, P.**, **Mielants, H.**, **CASPAR Study Group**, Classification criteria for psoriatic arthritis: Development of new criteria from a large international study. *Arthritis Rheum.* 2006. **54**: 2665–2673.

43 **Rudwaleit, M.**, **van der Heijde, D.**, **Landewé, R.**, **Listing, J.**, **Akkoc, N.**, **Brandt, J.**, **Braun, J. et al.**, The development of Assessment of SpondyloArthritis international Society classification criteria for axial spondyloarthritis (part II): validation and final selection. *Ann. Rheum. Dis.* 2009. **68**: 777–83.

44 **Livak, K. J. and Schmittgen, T. D.**, Analysis of relative gene expression data using real-time quantitative PCR and the 2(-Delta Delta C(T)) method. *Methods* 2001. **25**: 402–8.

45 **Benjamini, Y. and Hochberg, Y.**, Controlling the false discovery rate: a practical and powerful approach to multiple testing. *J. R. Stat. Soc. Ser. B.* 1995. **57**: 289–300.

46 **Li, Y.**, **Lip, G.**, **Chong, V.**, **Yuan, J. and Ding, Z.**, Idiopathic orbital inflammation syndrome with retro-orbital involvement: a retrospective study of eight patients rosenbaum JT, ed. *PLoS One* 2013. **8**: e57126.

47 **Yu, G.**, **Wang, L.-G.**, **Han, Y. and He, Q.-Y.**, clusterProfiler: an R package for comparing biological themes among gene clusters. *OMICS* 2012. **16**: 284–7.

48 **Kanehisa, M. and Goto, S.**, KEGG: kyoto encyclopedia of genes and genomes. *Nucleic Acids Res.* 2000. **28**: 27–30.

49 **Fabregat, A.**, **Jupe, S.**, **Matthews, L.**, **Sidiropoulos, K.**, **Gillespie, M.**, **Garapati, P.**, **Haw, R. et al.**, The reactome pathway knowledgebase. *Nucleic Acids Res.* 2018. **46**: D649–D655.

50 **Leek, J. T.**, **Scharpf, R. B.**, **Bravo, H. C.**, **Simcha, D.**, **Langmead, B.**, **Johnson, W. E.**, **Geman, D. et al.**, Tackling the widespread and critical impact of batch effects in high-throughput data. *Nat. Rev. Genet.* 2010. **11**: 733–9.

51 **Groeneveld, K. M.**, **Heeres, M.**, **Leenen, L. P. H.**, **Huisman, A. and Koenderman, L.**, Immunophenotyping of posttraumatic neutrophils on a routine haematology analyser. *Mediators Inflamm.* 2012. **2012**: 509513.

52 **ten Berg, M. J.**, **Huisman, A.**, **van den Bemt, P. M. L. A.**, **Schobben, A. F. A. M.**, **Egberts, A. C. G. and van Solinge, W. W.**, Linking laboratory and medication data: new opportunities for pharmacoepidemiological research. *Clin. Chem. Lab. Med.* 2007. **45**.

Abbreviations: **Crt**: cycle threshold (OpenArray) · **Ct**: cycle threshold (Single RT-qPCR assay) · **DLBCL**: diffuse large B cell lymphoma · **EMZL**: extranodal marginal zone lymphoma · **FC**: fold change · **HC**: healthy controls · **IOI**: idiopathic orbital inflammation · **miRNA**: microRNA · **NHOL**: non-Hodgkin orbital lymphoma · **RT-qPCR**: reverse transcription quantitative polymerase-chain reaction · **UPOD**: Utrecht patient orientated database

Full correspondence: Kamil G. Laban, Department of Ophthalmology, University Medical Center Utrecht, Room E 03.136, P.O. Box 85500, 3508 GA Utrecht, The Netherlands
e-mail: K.G.laban@umcutrecht.nl